$\mathcal{PT}$-symmetric coupler with a coupling defect: soliton interaction with exceptional point

Yuli V. Bludov,[1] Chao Hang,[2,5] Guoxiang Huang,[2] and Vladimir V. Konotop[3,4,6]

[1]*Centro de Física, Universidade do Minho, Campus de Gualtar, Braga 4710-057, Portugal*

[2]*State Key Laboratory of Precision Spectroscopy and Department of Physics, East China Normal University, Shanghai 200062, China*

[3]*Centro de Física Teórica e Computacional Faculdade de Ciêcias, Universidade de Lisboa, Instituto para Investigação Interdisciplinar, Avenida Professor Gama Pinto 2, Lisboa 1649-003, Portugal*

[4]*Departamento de Física, Faculdade de Ciêcias, Universidade de Lisboa, Campo Grande, Ed. C8, Piso 6, Lisboa 1749-016, Portugal*

[5]*e-mail: chang@phy.ecnu.edu.cn*

[6]*e-mail: vvkonotop@fc.ul.pt*

Received March 5, 2014; revised April 14, 2014; accepted April 15, 2014; posted April 16, 2014 (Doc. ID 207401); published June 3, 2014

We study the interaction of a soliton in a parity-time ($\mathcal{PT}$) symmetric coupler which has local perturbation of the coupling constant. This defect does not change the $\mathcal{PT}$-symmetry of the system, but locally can achieve the exceptional point. We found that the symmetric solitons after interaction with the defect either transform into breathers or blow up. The dynamics of antisymmetric solitons are more complex, showing domains of successive broadening of the beam and of the beam splitting in two outward propagating solitons, in addition to the single breather generation and blowup. All the effects are preserved when the coupling strength in the center of the defect deviates from the exceptional point. If the coupling is strong enough, the only observable outcome of the soliton-defect interaction is the generation of the breather.

OCIS codes: (190.5940) Self-action effects; (190.6135) Spatial solitons.

http://dx.doi.org/10.1364/OL.39.003382

Two coupled waveguides, with gain and losses that are mutually balanced are a parity-time ($\mathcal{PT}$)-symmetric system [1]. In the nonlinear case, [2] they represent a testbed for various phenomena involving instabilities and optical solitons. The couplers support stable propagation of bright [3–5] and dark [6] solitons, breathers [7], and rogue waves [8]. The dynamical properties of these systems are determined by the relation between the strengths of the coupling (κ) and the gain–loss coefficient (γ), splitting the region of the parameters into two domains. One domain corresponds to the unbroken $\mathcal{PT}$-symmetric phase, where all linear modes propagate without amplification or attenuation, and the other one corresponds to the broken $\mathcal{PT}$-symmetric phase, where the linear modes is unstable. The value of the relation γ/κ separating these two domains is an exceptional point (for a discussion of the physical relevance of exceptional points, see [9]).

When the coupling and gain/loss coefficient change along the propagation distance, the properties of the medium are affected and a new effect can be observed. In particular, the $\mathcal{PT}$-symmetry with an alternating sign can stabilize solitons [4]; a $\mathcal{PT}$-symmetric defect with localized gain and loss results in switching solitons between the waveguides [10]. The "governing" ratio γ/κ can also be changed by varying the coupling coefficient. This can be done by changing the properties of the medium between the waveguides or by using curved waveguides with varying distance between the waveguides. This situation was considered for conservative couplers in [11,12], where the local change of the coupling constant does not affect qualitatively the properties of the system. In the case of a $\mathcal{PT}$-symmetric coupler, however, if the change of κ locally reaches (or crosses) the exceptional point, the properties of the coupler are changed qualitatively. In this case, the $\mathcal{PT}$-symmetric phase is broken locally and we can speak about *exceptional point defect*.

We can expect that if the exceptional point defect is long enough (compared to the wavelength of soliton in the longitudinal direction), a soliton incident on it should become unstable. Indeed, in the spatial domain of the defect, a soliton cannot exist. Then we can expect different scenarios of the soliton instability. These scenarios are addressed in this Letter. More specifically, we study the interaction of a vector soliton in a $\mathcal{PT}$-symmetric coupler with the localized defect of coupling and report four possibilities of the soliton evolution interacting with the defect: the excitation of a one-period breather, the excitation of a breather with oscillating amplitude and width, the splitting of a vector soliton in two breathers, and the intensity blowup.

We consider two coupled waveguides described by two nonlinear Schrödinger equations

$$\begin{aligned} iq_{1,z} &= -q_{1,xx} + i\gamma q_1 - \kappa(z)q_2 - |q_1|^2 q_1, \\ iq_{2,z} &= -q_{2,xx} - i\gamma q_2 - \kappa(z)q_1 - |q_2|^2 q_2, \end{aligned} \tag{1}$$

with the coupling $\kappa = \kappa_0 - (\kappa_0 - \kappa_{\min})e^{-z^2/\ell^2}$, characterized by the amplitude $\kappa_0 - \kappa_{\min}$ (i.e., it attains the minimal value $\kappa_{\min}$ at $z = 0$ and tends to κ_0 at $z \to \pm\infty$) and by the width ℓ. To reduce the number of parameters, we set $\gamma = 1$ and leave as the only controlling parameters, the ones describing the coupling defect, i.e., κ_0, $\kappa_{\min}$, and ℓ. Respectively, $\kappa_{\min} = 1$ corresponds to the exceptional point defect.

In the limiting region where, $\kappa_{\min} \approx \kappa_0$, Eqs. (1) possess a soliton solution [3]:

$$q_1^{(\sigma)} = \frac{\sqrt{2}\eta \exp[i(\eta^2 + \sigma\kappa_0 \cos\delta)z]}{\cosh(\eta x)} = \sigma q_2^{(\sigma)} e^{-i\sigma\delta}, \tag{2}$$

where $\delta = \arcsin(\gamma/\kappa_0)$ such that $0 \le \delta \le \pi/2$. The soliton is parametrized by the positive parameter η, and represents symmetric ($\sigma = 1$) and antisymmetric ($\sigma = -1$) solutions. Equation (2) at $z = z_{\rm init}$ is used below for the initial data for vector solitons interacting with the defect.

Starting with the interaction of a symmetric soliton ($\sigma = 1$) with the exceptional point defect, $\kappa_{\min} = 1$, in Fig. 1 we present the typical results. The figure reveals the two different dynamical scenarios, which depend on whether the length of the defect ℓ is below or above some critical value ℓ_{cr}. In Fig. 1(a), the soliton passes through a relatively short defect transforming into a breather. The defect width in this case, $\ell = 1$, is far below the critical value: for $\eta = 0.15$, $\kappa_0 = 2$, and $\kappa_{\min} = 1$ we found $\ell_{cr} \approx 7$. The emergent breather solution is characterized by the intensity oscillations between the two components: minimum (maximum) in one component corresponds to maximum (minimum) in the other [Fig. 1(a)]. The frequency of these oscillations (after soliton passed the defect) can be estimated at $2\sqrt{\kappa_0^2 - \gamma^2}$. For the weak nonlinear limit, the estimate was derived in [7]. It stems from the difference of the eigenfrequencies of the linear $\mathcal{PT}$-symmetric coupler. At a finite amplitude the estimate for the frequency can be obtained from the following arguments. Introducing the Stokes variables $s_0 = |q_1|^2 + |q_2|^2$, $s_1 = q_1 q_2^* + q_1^* q_2$, $s_2 = -i(q_1 q_2^* - q_1^* q_2)$, and $s_3 = |q_1|^2 - |q_2|^2$, as well as their integrals $S_j = \int_{-\infty}^{\infty} s_j(z,x)\mathrm{d}x$, we obtain:

$$\frac{dS_0}{dz} = 2\gamma S_3, \qquad \frac{dS_2}{dz} = -2\kappa(z)S_3 + \int_{-\infty}^{\infty} s_1 s_3 \mathrm{d}x,$$
$$\frac{dS_1}{dz} = -\int_{-\infty}^{\infty} s_2 s_3 \mathrm{d}x, \qquad \frac{dS_3}{dz} = 2\gamma S_0 + 2\kappa(z)S_2.$$

For $\eta \ll 1$ we have $\int |q_j|^4 \mathrm{d}x \sim \eta^2 \int |q_j|^2 \mathrm{d}x$ and $|\int s_1 s_3 \mathrm{d}x| = |\int |q_1|^4 \mathrm{d}x - \int |q_2|^4 \mathrm{d}x| \ll |S_3|$. In this case, $\eta = 0.15$ and $\kappa_0 = 2$ and the nonlinear term in the equation for S_2 can be neglected with the accuracy $\eta^2/\kappa_0 \approx 0.011$. As a result, the system for S_0, S_2 and S_3 becomes closed and linear. One of its eigenfrequencies is $2\sqrt{\kappa_0^2 - \gamma^2}$, giving a period of oscillations $\pi/\sqrt{\kappa_0^2 - \gamma^2} \approx 1.8$; it agrees well with the numerical results in Fig. 1(a).

In Fig. 1(b), the solution passes through the same defect ($\ell = 1$) just below the critical value (for $\eta = 0.5$, $\kappa_0 = 4$, and $\kappa_{\min} = 1$ we found $\ell_{cr} \approx 1.1$) and is transformed into a breather. Now the period of oscillations is $\pi/\sqrt{\kappa_0^2 - \gamma^2} \approx 0.8$, which still agrees well with the numerical results. The dependencies of the total energy flow S_0 and the solution amplitudes $|q_{1,2}|$ on z for each case are shown in the lower panels. When the defect width is close to the threshold value (Fig. 1), the dependence $S_0(z)$ becomes quasiperiodic.

In Fig. 2, we show details of the evolution of the Stokes components and phases of the emergent breathers. The breathing character of the mode is evident from almost periodic power imbalance S_3 between the waveguides. We also observe that the breathing solution is accompanied by the oscillation of the "current" S_2 (which is constant for the soliton solution). These oscillations relate to

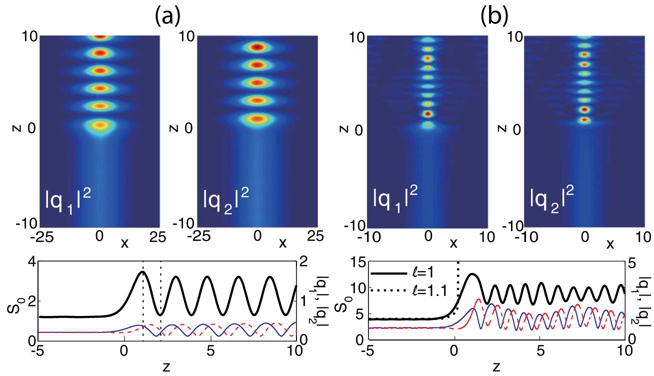

Fig. 1. Upper panels: field intensities with (a) $\eta = 0.15$ and (b) $\eta = 0.5$ interacting with defect at $z = 0$. The coupling $\kappa_{\min} = 1$, (a) $\kappa_0 = 2$ and (b) 4. Lower panels: respective evolution of the total energy flow S_0 for $\ell = 1$ (thick solid lines) and soliton amplitudes $|q_1|$ and $|q_2|$ (thin solid and dashed lines, respectively). The thick dotted line in (b) shows blowup at $\ell = 1.1$. The local maxima (minima) of S_0 [the vertical lines in the lower panel (a)] happen where the powers in the waveguides are equal: $\int |q_1|^2 \mathrm{d}x = \int |q_2|^2 \mathrm{d}x$. The simulations for bounded solutions have been performed between $z_{\rm ini} = -10$ and $z_{\rm fin} = 100$ and on the grid $-40 < x < 40$.

the lifting the phase locking between the components (Fig. 2): the phase difference $\theta = \arg q_1 - \arg q_2$, which is constant for soliton (2), in the breather solution depends periodically on the evolution coordinate. We also confirmed that the Stokes component S_1 remains much smaller than the other ones, what corroborates with the suppositions made in the estimates of the breather period.

If the length of the defect exceeds a critical value ℓ_{cr} for a given coupling constant, the soliton "cannot overcome" it. The component with gain q_1 (and hence S_0) grows infinitely. Thus the soliton after passing through the defect blows up [Fig. 1(b)]. We performed a detailed study of the dependence of the critical width of the defect ℓ_{cr} as a function of the minimal coupling $\kappa_{\min}$ [Fig. 3(a)]. The main qualitative result is that the exceptional point $\kappa_{\min} = 1$ separates quasi-linear (at $\kappa_{\min} < 1$) and quasi-exponential (at $1 < \kappa_{\min} < \kappa_{\min}^*$) dependencies $\ell_{cr}(\kappa_{\min})$.

Interestingly, when the $\mathcal{PT}$-symmetry is locally broken ($\kappa_{\min} < 1$) or even approaches zero, soliton still can pass the coupling defect, provided the defect is narrow enough. At the same time, the relatively strong coupling prevents a blowup. For $\kappa_{\min} > \kappa_{\min}^*$ there is no critical

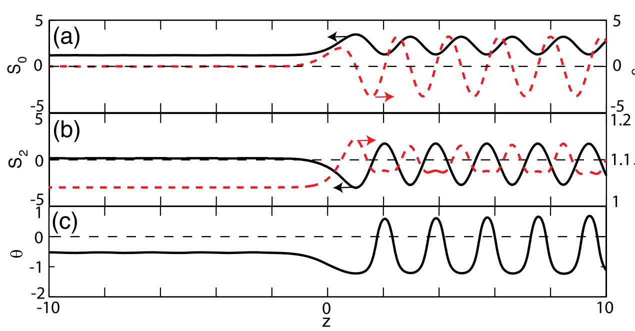

Fig. 2. (a) S_0 (solid line) and S_3 (dashed line) versus z, (b) S_2 (solid line) and S_1 (dashed line) versus z, and (c)"θ versus z. The parameters are the same with those used in Fig. 1(a).

width of a defect, and a soliton can pass a defect of *any* width being transformed in a breather. In the inset of Fig. 3(a) we show an example of strong coupling $\kappa_{\min} = 1.5$, where the defect with a sufficiently long width $\ell = 10$ results in the excitation of breathers. The blowup can occur in the whole interval of weak coupling $0 < \kappa_{\min} < \kappa_{\min}^*$ [in Fig. 3(a), $\kappa_{\min}^* \approx 1.5$].

In Fig. 3(b), we show the dependence of ℓ_{cr} on the inverse soliton width η at $\kappa_0 = 4$ and $\kappa_{\min} = 1$. For a given defect width there exists a critical soliton amplitude separating small amplitude solitons which pass the impurity being transformed in breathers and large amplitude solitons which blow up. We also observe an upper critical amplitude $\eta_{cr}^2 = 2\sqrt{\kappa_0^2 - 1}/3 \approx 1.6$, above which a soliton blows up independently of the width of the defect. This last effect is a manifestation of the instability of the large amplitude solitons in a $\mathcal{PT}$-symmetric coupler [3]. As in the previous case, solitons with $\eta < \eta^* \approx 0.1$ are able to pass the defect of any width without blowing up. In the inset of Fig. 2(b), we show an example of the excitation of a breather by small amplitude solitons.

Turning to the interaction of the antisymmetric soliton $\sigma = -1$ with an exceptional point defect we observe more rich behavior, which is presented in Fig. 4. As in the case of a symmetric soliton, we find that there exists a critical defect length ℓ_{cr} above which the soliton blows up (for the chosen parameters $\ell_{cr} \approx 3.4$). If the width of the defect is below ℓ_{cr}, the soliton-defect interaction results in the creation of breathers, although this occurs now according to different scenarios. The effect of a relatively short defect acts similarly on the symmetric and antisymmetric solitons, cf. panels (a) in Figs. 1 and 4. Here one observes that the antisymmetric breathers have a shorter period (≈ 0.8) than that of the symmetric ones.

The increase of the defect lengths results in the broadening of the soliton past the defect [Fig. 4(b)]. This broadening is repeated along the propagation distance in Fig. 4(b) the period ≈ 10. The further increase of ℓ leads to the splitting of the incident soliton in the two outward propagating pulses, as it is shown in Fig. 4(c). It turns out that the domain of the defect lengths leading to the splitting of the incident beam is finite (for the parameters of Fig. 4 this is the domain $2.2 \le \ell \le 3.2$). Interestingly, the further increasing of the defect length stops soliton splitting and reintroduces the scenario when broadening of

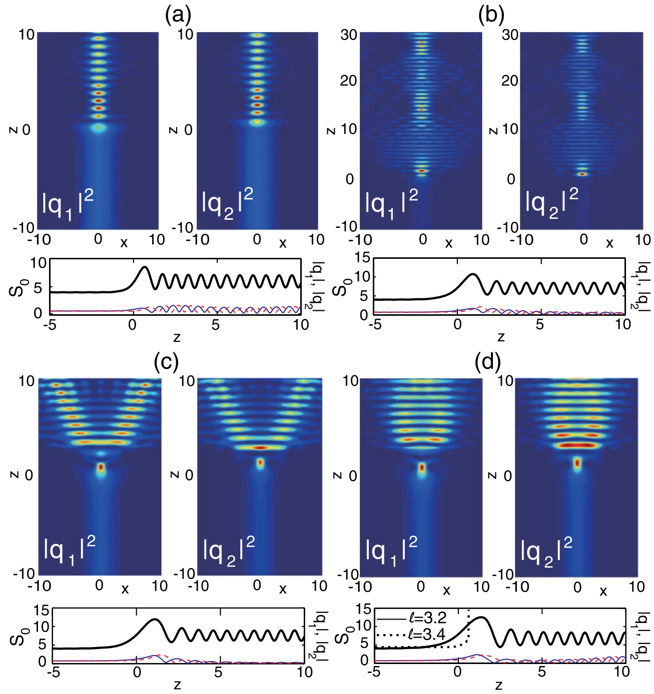

Fig. 4. Upper panels: The dynamics of soliton-defect interactions for (a) $\eta = 0.5$ and $\ell = 1.1$, (b) 2.2, (c) 2.7, and (d) 3.2, respectively, for the coupling $\kappa_0 = 4$ and $\kappa_{\min} = 1$. In (a) and (b), the broadening is repeated along the propagation distance with the period ≈ 10. Lower panels: The total energy flow S_0 (thick solid lines) and soliton amplitudes $|q_1|$ and $|q_2|$ (thin solid and dashed lines, respectively) for each solution. The thick dotted line in (d) corresponds to the blow up happening at $\ell = 3.4$.

the soliton is observed [Fig. 4(d)]. In spite of the reported diversity of the behaviors, the total energy flow S_0 is increasing smoothly with the growth of ℓ displaying no reflection of the broadening or splitting dynamics.

In Fig. 5, we show (a) ℓ_{cr} versus $\kappa_{\min}$ and (b) ℓ_{cr} versus η for $\kappa_{\min} = 1$ for the case of antisymmetric soliton. Comparing Figs. 5 and 3, we observe that the blowup of a symmetric soliton occurs at lower amplitudes and smaller defect lengths than the blowup of an antisymmetric soliton.

The interactions of the solitons of both types with the defect obey several common features. First, the soliton-defect interaction starts with the local increase of the

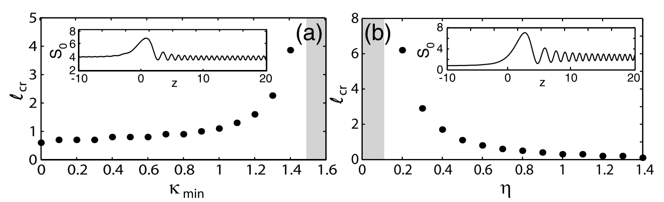

Fig. 3. Dependencies of ℓ_{cr} versus $\kappa_{\min}$ for $\eta = 0.5$ (a) and versus η for $\kappa_{\min} = 1$ (b). In both panels $\kappa_0 = 4$. If $\kappa_{\min} > \kappa_{\min}^* \approx 1.5$ (a) and $\eta < \eta^* \approx 0.1$ (b) (the gray domains) no blowup is found under the given values of the parameters. Insets show the dynamics of Stokes components (a) for a soliton interacting with a strong coupling defect $\kappa_{\min} = 1.5$ and (b) for a small amplitude soliton ($\eta = 0.1$) interacting with the exceptional point defect, where a sufficiently long defect, $\ell = 10$, results in the excitation of a breather.

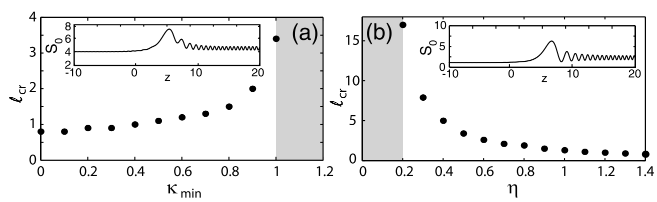

Fig. 5. (a) ℓ_{cr} versus $\kappa_{\min}$ for $\eta = 0.5$ and (b) ℓ_{cr} versus η for $\kappa_{\min} = 1$. In both panels $\kappa_0 = 4$. If (a) $\kappa_{\min} > \kappa_{\min}^* \approx 1$ and (b) $\eta < \eta^* \approx 0.2$ (the gray domains), no blowup occurs for the given parameters. The insets show the Stokes components for the defect with (a) $\kappa_{\min} = 1.1$ and (b) for the small amplitude soliton ($\eta = 0.1$) interacting with the exceptional point defect, where the defect of the length $\ell = 10$ results in the excitation of breathers.

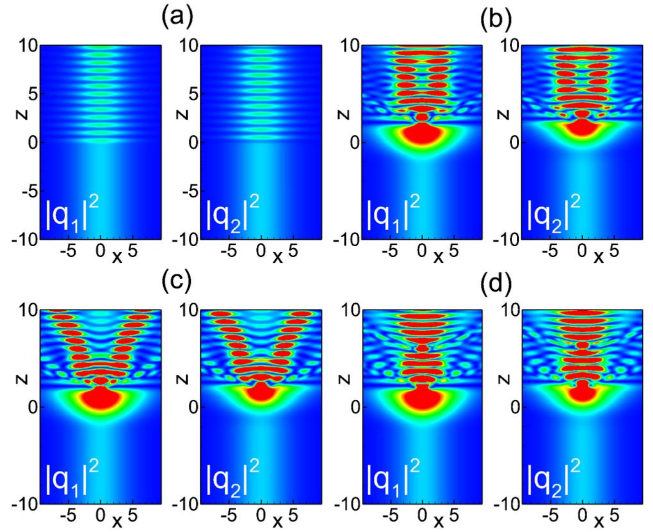

Fig. 6. Soliton interaction with super-Gaussian defect for (a) $\eta = 0.25$, $\kappa_0 = 4$, $\kappa_{\min} = 1$ and $\ell = 0.2$; (b) $\ell = 2.0$; (c) $\ell = 2.1$; and (d) $\ell = 2.2$.

energy flow. Indeed, the initial (solitonic) values of the Stokes parameters are given by: $S_0^{(s)} = 8\eta$, $S_1^{(s)} = 8\eta\sigma \cos\delta$, $S_2^{(s)} = -8\eta \sin\delta$, $S_3^{(s)} = 0$ ($s_3 \equiv 0$) and thus (3) gives that at the initial stage of evolution S_0 and S_3 are growing independently of defect parameters. Second, it follows from (3) that for an *exact* breathing, i.e., L-periodic, solution $\langle S_3 \rangle = (1/L)\int_z^{z+L} S_3(z)\mathrm{d}z = 0$. For a breather far from the defect, where $\kappa(z) \approx \kappa_0$, we also find that $\langle S_2 \rangle = -(\gamma/\kappa)\langle S_0 \rangle < 0$. Thus, the defect results in oscillations of $S_2(z)$ without changing the sign of its average.

Finally, using the super-Gaussian defect $\kappa = \kappa_0 - (\kappa_0 - \kappa_{\min})e^{-z^6/\ell^6}$, we checked the sensitivity of our results to the choice of the defect. We found that for the parameters as in Fig. 1(b) the critical value becomes $\ell_{cr} \approx 0.5$. For the antisymmetric mode, the results are shown in Fig. 6. We observe that there are the same scenarios as those in Fig. 4 (although now $\ell_{cr} \approx 2.3$ for $\eta = 0.25$). It is interesting that for $\eta = 0.5$, the critical value $\ell_{cr} \approx 1.1$, i.e., considerably lower than the one established in Fig. 4.

In conclusion, we considered the interaction of a diffractive soliton in a $\mathcal{PT}$-symmetric coupler with a coupling defect, which locally achieves the exceptional point of the underline linear system. Independent of whether the incident beam (soliton) is symmetric or antisymmetric, at relatively small defect length the soliton passes through the defect and transforms into a breather. This occurs even if in the region of the defect the $\mathcal{PT}$-symmetry is broken. If the defect is long enough, the total energy flow grows exponentially along the waveguides. In the case of an antisymmetric soliton interacting with a defect there domains van exist where successive broadening of the beam and even beam splitting in two outward propagating breathers occurs.

The work was supported by the Program of Introducing Talents of Discipline to Universities under Grant No. B12024. Y. V. B. and V. V. K. were supported by FCT (Portugal) grants PEst-C/FIS/UI0607/2013, PEst-OE/FIS/UI0618/2011, PTDC/FIS-OPT/1918/2012. C. H. and G. X. H. were supported by the NSF-China grants 11105052 and 11174080.

References

1. C. E. Rüter, K. G. Makris, R. El-Ganainy, D. N. Christodoulides, M. Segev, and D. Kip, Nat. Phys. **6**, 192 (2010).
2. H. Ramezani, T. Kottos, R. El-Ganainy, and D. N. Christodoulides, Phys. Rev. A **82**, 043803 (2010).
3. R. Driben and B. A. Malomed, Opt. Lett. **36**, 4323 (2011).
4. R. Driben and B. A. Malomed, Europhys. Lett. **96**, 51001 (2011).
5. N. V. Alexeeva, I. V. Barashenkov, A. A. Sukhorukov, and Y. S. Kivshar, Phys. Rev. A **85**, 063837 (2012).
6. Y. V. Bludov, V. V. Konotop, and B. A. Malomed, Phys. Rev. A **87**, 013816 (2013).
7. I. V. Barashenkov, S. V. Suchkov, A. A. Sukhorukov, S. V. Dmitriev, and Y. S. Kivshar, Phys. Rev. A **86**, 053809 (2012).
8. Y. V. Bludov, R. Driben, V. V. Konotop, and B. A. Malomed, J. Opt. **15**, 064010 (2013).
9. W. D. Heiss, J. Phys. A **45**, 44016 (2012).
10. F. K. Abdullaev, V. V. Konotop, M. Ögren, and M. P. Sørensen, Opt. Lett. **36**, 4566 (2011).
11. P. L. Chu, B. A. Malomed, G. D. Peng, and I. M. Skinner, Phys. Rev. E **49**, 5763 (1994).
12. I. M. Skinner, G. D. Peng, B. A. Malomed, and P. L. Chu, Opt. Commun. **113**, 493 (1995).